

Strain partition of Si/SiGe and SiO₂/SiGe on compliant substrates

H. Yin^{a)}

*Center for Photonics and Optoelectronic Materials and Department of Electrical Engineering,
Princeton University, Princeton, New Jersey 08544*

K. D. Hobart and F. J. Kub

Naval Research Laboratory, Washington, DC 20375

S. R. Shieh and T. S. Duffy

Department of Geosciences, Princeton University, Princeton, New Jersey 08544

J. C. Sturm

*Center for Photonics and Optoelectronic Materials and Department of Electrical Engineering,
Princeton University, Princeton, New Jersey 08544*

(Received 13 January 2003; accepted 27 March 2003)

Strain partitioning of crystalline Si and amorphous SiO₂ deposited on crystalline SiGe on a compliant viscous borophosphosilicate (BPSG) glass has been observed. Pseudomorphic epitaxial Si was deposited on SiGe films, which were fabricated on BPSG by wafer bonding and the Smart-cut® process. The strains in SiGe and Si films were found to change identically during a high-temperature anneal which softened the BPSG film, indicating a coherent interface between SiGe and Si films and precluding slippage or the formation of misfit dislocations along the interface. The stress balance between the layers dictated the final state, which confirmed that BPSG was a perfectly compliant substrate and did not exert any force on the layers above it. Similar results were found for amorphous SiO₂ deposited on SiGe on BPSG and then annealed. This shows that the viscous BPSG is an effective compliant substrate for the strain engineering of elastic films without the introduction of dislocations. © 2003 American Institute of Physics.

[DOI: 10.1063/1.1578168]

The integration of lattice-mismatched materials has motivated the development of compliant substrates.¹ The ideal compliant substrate structure allows a crystalline thin film above to expand or shrink, thus reducing the strain energy in the system, without the formation of defects such as dislocations. This provides a template for subsequent epitaxy with an in-plane lattice constant different than that of the original substrate. A variety of methods have been utilized to realize compliant substrates, with most of them trying to form a thin template layer that decouples the thick substrates from top epitaxial layers grown later.^{2–10} In practice, pseudomorphic strained layers are often grown on top of these templates, and the whole structure is then annealed to further adjust the lattice constant. Ideally, this relaxation step is accomplished without dislocations (e.g., at the interface between the template and the top layer) so that all layers remain coherent, as has been commonly assumed in many compliant substrate studies.^{1,11–14} However, in the case where such a structure has been examined in detail, coherence was not observed,¹⁵ leading to uncertainty about the nature of the compliance mechanism. In this letter, we clearly show a coherent relation of bilayers on a compliant substrate of a thin borophosphosilicate (BPSG) film. This work shows that dislocations are not inherently included in the relaxation of layers on these compliant BPSG films.

Consider two layers on top of a compliant substrate (Fig. 1). When the strain energy is minimized by the coherent displacement of the top two layers and the compliant sub-

strate [Fig. 1(a)], the introduction of dislocations or other kinds of defects is not required. The original strain is partitioned between layers. When the strain energy in the system is reduced by dislocation formation [Fig. 1(b)], there are no longer coherent interfaces between layers. The compliance, however, manifests itself by modifying dislocation dynamics.¹⁶ The fact that dislocations render interfaces incoherent between layers suggests that strain partitioning in layers on a compliant substrate is a key test on the mechanism of compliance. Without clear evidence of strain partitioning, it has been suspected that some approaches of compliant substrates in III–V materials actually take advantage of the change in dislocation dynamics.^{15,17}

The recent application of viscous BPSG as a compliant substrate has yielded high-quality fully relaxed Si_{0.7}Ge_{0.3} films.^{18,19} A 30 nm Si_{0.7}Ge_{0.3} film commensurately strained to bulk Si(100) is transferred to a 200 nm BPSG film (a viscosity of 1.2×10^{10} N s/m at 800 °C) on a Si wafer by a wafer bonding, Smart-cut® and etch-back process, and then patterned to islands. When the anneal temperature is elevated to 800 °C, the BPSG film softens and the as-bonded, compressively strained SiGe film starts to relax by macroscopic expansion. Transmission electron microscopy examination has indicated that the dislocation density is low and, therefore, suggested that the underlying relaxation mechanism is indeed the expansion of SiGe layers on viscous BPSG films.¹⁹

Epitaxial Si, Si_{0.7}Ge_{0.3} and amorphous SiO₂ are the elastic films studied in the strain partition tests. The highest anneal temperature used is 850 °C, well below the glass transition point of SiO₂.²⁰ Therefore, it is safe to treat all films as

^{a)}Electronic mail: hyin@ee.princeton.edu

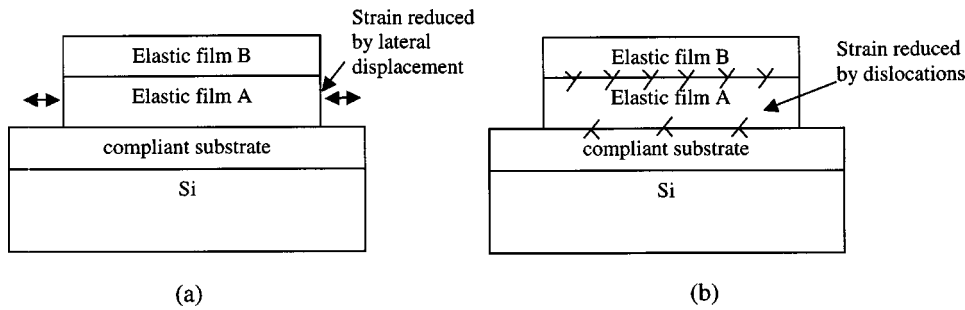


FIG. 1. Schematic diagram of compliance mechanisms. (a) Strain energy is minimized by lateral displacement of the elastic layers and the compliant substrate. Coherent interfaces between them are retained. (b) Strain energy is reduced by the formation of dislocations, which render the interfaces incoherent. (Dislocations are only relevant at the lower interface for crystalline compliant substrate.)

elastic ones in this study. These films are patterned into square islands of various sizes by reactive ion etching to allow for lateral macroscopic expansion. Micro-Raman spectroscopy was used to locally measure the strain in $\text{Si}_{0.7}\text{Ge}_{0.3}$ and Si films.¹⁹

In this letter, the coherent relaxation of different samples of four structure types on BPSG is observed. In the first experiment, a compressively strained $\text{Si}_{0.7}\text{Ge}_{0.3}$ (30 nm, strain $\varepsilon_0 = -1.2\%$) on relaxed Si (25 nm) was first transferred to BPSG and patterned into $30\ \mu\text{m}$ islands (Fig. 2 inset). Upon annealing at $800\ ^\circ\text{C}$ in nitrogen to reduce the viscosity of BPSG and thus remove the mechanical constraint from the substrate, the compressively strained SiGe layer expands to lessen the strain and the Si layer is stretched to become tensile (Fig. 2). The fact that the same increase in strain ($\sim 0.6\%$) is seen in both layers clearly implies an absence of slippage or misfit dislocations between the Si and SiGe layers. Further, one can predict the final strains of the annealed samples by the stress balance between the layers:

$$\sigma_{\text{SiGe}}h_{\text{SiGe}} + \sigma_{\text{Si}}h_{\text{Si}} = 0, \quad (1)$$

where σ represents film stress under equal biaxial stresses ($\sigma_{11} = \sigma_{22} = \sigma$) and h refers to the thickness of the film. Along with the assumption of a coherent interface between the Si and SiGe layers, Eq. (1) predicts:

$$\varepsilon_{\text{SiGe}} = \varepsilon_0 \frac{(1 - \nu_{\text{SiGe}})E_{\text{Si}}h_{\text{Si}}}{(1 - \nu_{\text{Si}})E_{\text{SiGe}}h_{\text{SiGe}} + (1 - \nu_{\text{SiGe}})E_{\text{Si}}h_{\text{Si}}}, \quad (2)$$

$$\varepsilon_{\text{Si}} = -\varepsilon_0 \frac{(1 - \nu_{\text{Si}})E_{\text{SiGe}}h_{\text{SiGe}}}{(1 - \nu_{\text{Si}})E_{\text{SiGe}}h_{\text{SiGe}} + (1 - \nu_{\text{SiGe}})E_{\text{Si}}h_{\text{Si}}}. \quad (3)$$

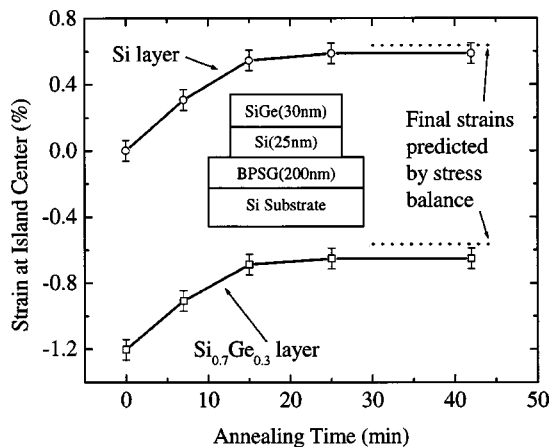


FIG. 2. Coherent strain evolution of Si and $\text{Si}_{0.7}\text{Ge}_{0.3}$ films as they reach stress equilibrium during an anneal at $800\ ^\circ\text{C}$. The strains are measured at the center of a $30\ \mu\text{m} \times 30\ \mu\text{m}$ island. The final equilibrium state agrees with the predicted stress balance between Si and $\text{Si}_{0.7}\text{Ge}_{0.3}$ films, depicted by the dotted lines.

E and ν refer to the Young's Modulus and Poisson's ratio of the film, respectively, whose values are listed in Table I. The good agreement of the observed final strains with the predictions by stress balance is further evidence of the relaxation by compliant BPSG without dislocations.

A second experiment was performed to verify that the stress balance between the layers governs the mechanical equilibrium. Epitaxial unstrained Si of various thicknesses was grown at $700\ ^\circ\text{C}$ by rapid thermal chemical vapor deposition (RT-CVD) on a compressively strained 30 nm $\text{Si}_{0.7}\text{Ge}_{0.3}$ layer on BPSG before relaxation (Fig. 3 inset). This structure was patterned to $30\ \mu\text{m}$ square islands and then annealed in nitrogen at $800\ ^\circ\text{C}$ long enough to reach mechanical equilibrium (1 to 3 h). Figure 3 shows the final equilibrium strains in the two layers as a function of the top Si thickness, both experimentally measured and also predicted by stress balance [Eqs. (2) and (3)]. Again, excellent agreement was observed.

Up to this point, the strain partition has been examined only during the lateral expansion of elastic layers. To demonstrate the full capability of strain engineering using the viscous BPSG film, the lateral shrinkage of elastic layers during the stress balance process was also examined. In a third experiment, $30\ \mu\text{m}$ square islands of 30 nm $\text{Si}_{0.7}\text{Ge}_{0.3}$ on BPSG were first almost fully relaxed at $800\ ^\circ\text{C}$. A 30 nm Si layer was commensurately and selectively deposited on the relaxed $\text{Si}_{0.7}\text{Ge}_{0.3}$ islands by RT-CVD (Fig. 4 inset). The measured tensile strain in the Si layer was about 1.1%, as expected for pseudomorphic epitaxial Si on relaxed $\text{Si}_{0.7}\text{Ge}_{0.3}$. This structure was annealed for 1 h at $800\ ^\circ\text{C}$ in nitrogen to reach equilibrium (Fig. 4). Again, the stress balance accurately predicts the final strains.

Note that in all three cases described so far, the $\text{Si}_{0.7}\text{Ge}_{0.3}$ thicknesses were above the critical thickness not only for a single thin film on a bulk Si substrate ($\sim 8\ \text{nm}$), but also for that predicted in a free-standing Si/ $\text{Si}_{0.7}\text{Ge}_{0.3}$ bilayer (maximum critical thickness $\sim 16\ \text{nm}$ for Si thickness $> 16\ \text{nm}$ in Ref. 12). Thus, dislocations might have been expected by thermodynamic considerations. The fact that the two layers relaxed together in all cases emphasizes the compliant nature of the substrate and that the strain in layers relaxes more

TABLE I. Mechanical properties^a of Si and $\text{Si}_{0.7}\text{Ge}_{0.3}$ (linearly interpolated between Si and Ge).

$E(\text{Si}_{0.7}\text{Ge}_{0.3})$ ($10^{10}\ \text{N/m}^2$)	$E(\text{Si})$ ($10^{10}\ \text{N/m}^2$)	$\nu(\text{Si}_{0.7}\text{Ge}_{0.3})$	$\nu(\text{Si})$
12.2	13.0	0.28	0.28

^aSee Ref. 21.

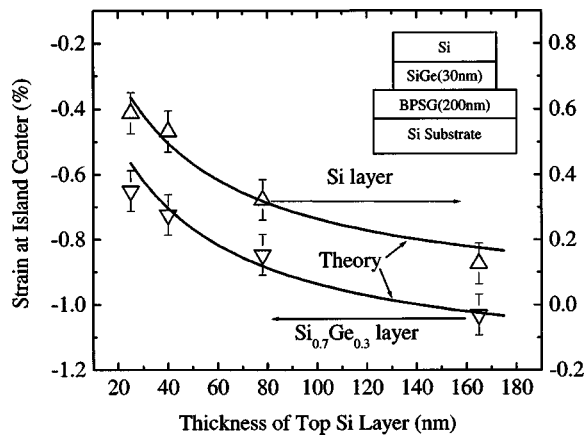


FIG. 3. Biaxial strains of 30 nm $\text{Si}_{0.7}\text{Ge}_{0.3}$ and Si at the center of a $30\ \mu\text{m} \times 30\ \mu\text{m}$ island as a function of Si thickness after anneals at $800\ ^\circ\text{C}$ to reach equilibrium. Open symbols are experimental data. Lines are calculation of stress balance based on the elastic parameters in Table I.

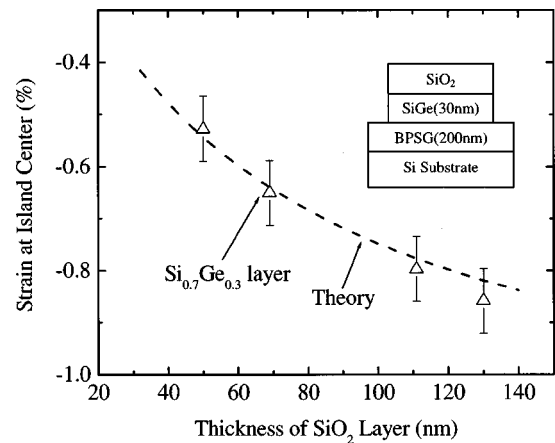


FIG. 5. Biaxial strain of the initially compressively strained 30 nm $\text{Si}_{0.7}\text{Ge}_{0.3}$ at the center of a $30\ \mu\text{m} \times 30\ \mu\text{m}$ island, after deposition of PECVD SiO_2 and an anneal, as a function of PECVD- SiO_2 thickness. Open symbols are experimental data and the dashed line is a fitting based on stress balance.

quickly through lateral expansion or contraction enabled by the viscous flow of the compliant substrate than through dislocation formation.

Finally, we show the stress balance with a deposited amorphous oxide layer, instead of epitaxial, crystalline layers. A SiO_2 layer was deposited on a compressively strained 30 nm $\text{Si}_{0.7}\text{Ge}_{0.3}$ layer on BPSG by plasma-enhanced chemical vapor deposition (PECVD) at $250\ ^\circ\text{C}$. The SiO_2/SiGe stack was patterned to $30\ \mu\text{m}$ square islands and was then annealed at $800\ ^\circ\text{C}$ for 2 h to reach an equilibrium state (Fig. 5 inset). Due to the difficulty in measuring the strain in the oxide layer on a small island, only the strain in SiGe layer was measured (Fig. 5). It is observed that thicker oxides impede the relaxation of the SiGe. The data were modeled assuming the stress balance. This gives rise to the dashed line in Fig. 5 with a single fitting parameter of $E_{\text{oxide}}/1 - \nu_{\text{oxide}}$ chosen for best fit ($8.5 \times 10^{10}\ \text{N/m}^2$), because this ratio varies in SiO_2 . Again, good agreement with the stress balance was observed, implying the SiGe relaxed only through lateral expansion and not via dislocations.

In summary, we have confirmed coherent interfaces and strain partitioning in Si/SiGe and SiO_2/SiGe on viscous BPSG films. Governed by the stress balance, the layers can

either shrink or expand on the viscous BPSG to minimize the strain energy. The formation of dislocations is unnecessary in this process. Thus, the viscous films, such as a BPSG film, are a promising compliant substrate for defect-free strain engineering of lattice-mismatched films.

The authors appreciate helpful discussions with Z. Suo, R. Huang, and J. Liang. This work is supported by DARPA (N66001-00-10-8957).

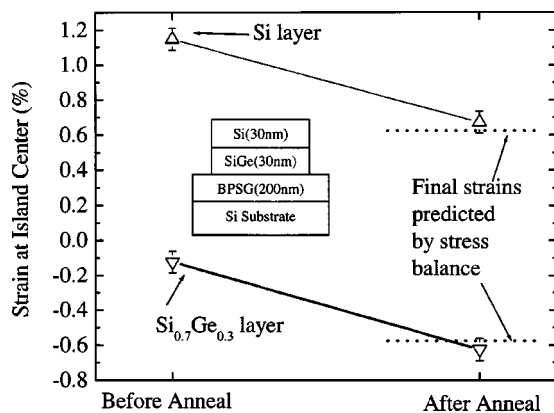


FIG. 4. Biaxial strain of $\text{Si}_{0.7}\text{Ge}_{0.3}$ and Si at the center of an initially relaxed $30\ \mu\text{m} \times 30\ \mu\text{m}$ $\text{Si}_{0.7}\text{Ge}_{0.3}$ island before and after an anneal. Open symbols are experimental data and dotted lines are calculation of stress balance.

- ¹ Y. H. Lo, Appl. Phys. Lett. **59**, 2311 (1991).
- ² A. R. Powell, S. S. Lyer, and F. K. LeGoues, Appl. Phys. Lett. **64**, 1856 (1994).
- ³ Z. Yang, F. Guarin, I. W. Tao, W. I. Wang, and S. S. Lyer, J. Vac. Sci. Technol. B **13**, 789 (1995).
- ⁴ D. M. Follstaedt, S. M. Jyers, and S. R. Lee, Appl. Phys. Lett. **69**, 2059 (1996).
- ⁵ F. E. Ejeckam, Y. H. Lo, S. Subramanian, H. Q. Hou, and B. E. Hammons, Appl. Phys. Lett. **71**, 776 (1997).
- ⁶ S. I. Romanov, V. I. Mashanov, L. V. Sokolov, A. Gutakovskii, and O. P. Pchelyakov, Appl. Phys. Lett. **75**, 4118 (1999).
- ⁷ S. Mantl, B. Hollaender, R. Liedtke, S. Mesters, H. J. Herzog, H. Kibbel, and T. Hackbarth, Nucl. Instrum. Methods Phys. Res. B **147**, 29 (1999).
- ⁸ P. D. Moran, D. M. Hansen, R. J. Matyi, J. G. Cederberg, L. J. Mawst, and T. F. Kuech, Appl. Phys. Lett. **75**, 1559 (1999).
- ⁹ F. Y. Huang, M. A. Chu, M. O. Tanner, K. L. Wang, G. D. U'Ren, and M. S. Goorsky, Appl. Phys. Lett. **76**, 2680 (2000).
- ¹⁰ Y. H. Luo, J. Wan, R. L. Forrest, J. L. Liu, M. S. Goorsky, and K. L. Wang, J. Appl. Phys. **89**, 8279 (2001).
- ¹¹ D. Teng and Y. H. Lo, Appl. Phys. Lett. **62**, 43 (1993).
- ¹² L. B. Freund and W. D. Nix, Appl. Phys. Lett. **69**, 173 (1996).
- ¹³ C. Carter-Coman, R. Bicknell-Tassius, A. S. Brown, and N. M. Joerst, Appl. Phys. Lett. **71**, 1344 (1997).
- ¹⁴ D. Zubia, S. D. Hersee, and T. Khraishi, Appl. Phys. Lett. **80**, 740 (2002).
- ¹⁵ P. D. Moran, D. M. Hansen, R. J. Matyi, L. J. Mawst, and T. F. Kuech, Appl. Phys. Lett. **76**, 2541 (2000).
- ¹⁶ C. W. Pei, B. Turk, W. I. Wang, and T. S. Kuan, J. Appl. Phys. **90**, 5959 (2001).
- ¹⁷ G. Kastner and U. Gösele, J. Appl. Phys. **88**, 4048 (2000).
- ¹⁸ K. D. Hobart, F. J. Kub, M. Fatemi, M. E. Twigg, P. E. Thompson, T. S. Kuan, and C. K. Inoki, J. Electron. Mater. **29**, 897 (2000).
- ¹⁹ H. Yin, R. Huang, K. D. Hobart, Z. Suo, T. S. Kuan, C. K. Inoki, S. R. Shieh, T. S. Duffy, F. J. Kub, and J. C. Sturm, J. Appl. Phys. **91**, 9716 (2002).
- ²⁰ K. Nassau, R. A. Levy, and D. L. Chadwick, J. Electrochem. Soc. **132**, 209 (1985).
- ²¹ M. Newberger, Handbook of Electronic Materials, Group IV Semiconducting Materials Vol. 5 (IFI/Plenum, New York, 1971).